Research Article

Hoang Nguyen Khac*, Amin Modabberian, Xiaoguo Storm, Kai Zenger and Jari Hyvönen

# Model predictive control for a multiple injection combustion model

https://doi.org/10.1515/eng-2021-0113
received May 15, 2021; accepted October 26, 2021

**Abstract:** In this work, a model predictive controller is developed for a multiple injection combustion model. A 1D engine model with three distinct injections is used to generate data for identifying the state-space representation of the engine model. This state-space model is then used to design a controller for controlling the start of injection and injected fuel mass of the post injection. These parameters are used as inputs for the engine model to control the maximum cylinder pressure and indicated mean effective pressure.

**Keywords:** model predictive control, identification for control, data-driven control, multiple injection

## 1 Introduction

International emission regulations (e.g., Tier III, China II) are becoming stricter every year, which sets more challenges on combustion engines. In some industries, such as maritime, no replacement of combustion engines can be foreseen in the near future due to high demand of the large energy efficiency. There is a need for new efficient use of renewable fuels and new low-temperature combustion technologies that would reduce the harmful emissions.

Lowering the emissions excessively under the legislation limits would increase the engine operating costs such as higher fuel consumption [1]. The challenge is to fulfill the emission standards and to maximize the engine efficiency. Overcoming this problem requires more advanced combustion control than the traditional engine tuning and calibration. There have been several new approaches in the engine combustion control, which are based on new low-temperature combustion technologies, e.g., reactivity controlled compression ignition, homogeneous charge compression ignition, and partially premixed combustion. Control in these is complicated however, and they are based on controlling the cylinder pressure by several successive fuel injections during each engine cycle. Engine efficiency can be increased by maintaining the cylinder pressure at its highest level throughout the combustion [2]. Multiple injection strategy is one of the new methods being used to maximize the cylinder pressure. It is an alternative approach to single injection combustion, which has been proved to be more efficient in terms of noise and emission reduction, and fuel consumption [3]. The multiple injection enables better control of the fuel distribution [4].

In this work, a model predictive control (MPC) is applied for multiple injection strategy in a maritime diesel engine. The aim is to predict and control the engine combustion parameters cycle-to-cycle. The MPC controller is designed based on a state-space representation of the combustion process. The model is obtained by data-driven method from a multiple injection combustion model.

The reason for choosing the MPC method is upon its ability to solve the optimization problem using a moving time horizon window [5], which can be considered as the working cycle of the cylinder. In this problem, the MPC is controlling the fuel injection parameters under constraints such as the maximum cylinder pressure value. The optimization problem is to maximize the cylinder pressure and the indicated mean effective pressure (IMEP) over a cycle.

## 2 Engine model

The model used in this work to generate data for system identification is a 1D model based on a 4-cylinder, 4 stroke, 2L diesel engine with direct injection provided

* **Corresponding author: Hoang Nguyen Khac,** Department of Electrical Engineering and Automation, Aalto University, Maarintie 8, Espoo, Finland, e-mail: hoang.kh.nguyen@aalto.fi
**Amin Modabberian:** Department of Electrical Engineering and Automation, Aalto University, Maarintie 8, Espoo, Finland, e-mail: amin.modabberian@aalto.fi
**Xiaoguo Storm:** Department of Energy Technology, School of Technology and Innovations, University of Vaasa, Vaasa, Finland, e-mail: xxue@uwasa.fi
**Kai Zenger:** Department of Electrical Engineering and Automation, Aalto University, Aalto, Finland, e-mail: kai.zenger@aalto.fi
**Jari Hyvönen:** Research and Development, Internal Combustion Engines Department, Vaasa, Finland, e-mail: jari.hyvonen@wartsila.com

by Gamma Technologies [6]. The engine model is created with GT-suite integrated simulation environment. The combustion model of the engine is developed with DI-pulse method, a predictive combustion model that utilizes detailed injection profiles. The injection profiles are generated using a detailed injector model developed by Payri et al. [7]. The in-cylinder heat transfer is modeled with Woschni model and temperatures of cylinder, head, and piston are modeled with a finite-element model.

DI-pulse is a phenomenological combustion model developed by Gamma Technologies. It provides the possibility to predict the parameters associated with in-cylinder combustion and emission for single and multiple injection strategies. The model divides the cylinder into three thermodynamic zones. These zones are the unburned zone, the unburned spray zone, and the spray burned zone, each zone having distinct temperature and composition. The unburned zone contains the trapped air mass at intake valve closing, the unburned spray zone contains injected fuel and entrainment mass, and the burned spray mass contains combustion products. GT-power uses different models for the different phases of the combustion. These phases are fuel injection, entrainment model, evaporation, ignition delay, premixed combustion, and diffusion combustion. Four latter phases have their own coefficient that has a great impact on that particular phase. In addition to DI-pulse, the utilized model demonstrates other essential concepts of diesel engines such as variable geometry turbine, boost control, intercooler, exhaust gas recirculation (EGR) circuit with cooler and EGR rate control, injection limiting for control, and geometry only exhaust after treatment device modeling [8].

The reason of using a simulation model for data generation is that phenomenological models provide accurate results for control design purposes in the absence of data generated by a real engine.

## 2.1 Fuel injection

Each injection is defined as a separate pulse and is tracked and added separately to the unburned spray zone as shown in Figure 1. Number of pulses in DI-pulse is unlimited, although in both simulation and real engine applications that is not possible. Additionally, there is no distinction made between pilot, main, and post injection pulses.

The length of spray penetration at time $t$ for each injection pulse is calculated in equation (1)

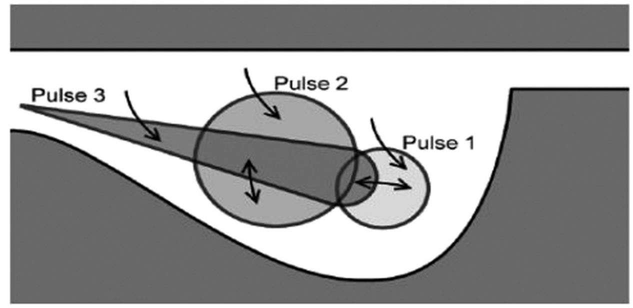


**Figure 1:** Illustration of injection pulses [8].

$$S = \begin{cases} u_{\text{inj}} t \left( 1 - \frac{1}{16} \left( \frac{t}{t_b} \right)^8 \right), & \text{when } \frac{t}{t_b} \le 1 \\ u_{\text{inj}} t_b (1 - \frac{15}{16} \left( \frac{t}{t_b} \right)^5 ), & \text{when } \frac{t}{t_b} \ge 1, \end{cases} \quad (1)$$

where $u_{\text{inj}}$ is the injection velocity at injector nozzle and $t_b$ is the breakup time of spray into droplets. The velocity $u_{\text{inj}}$ and breakup time $t_b$ are defined in equations (2) and (3), respectively

$$u_{\text{inj}} = C_d \sqrt{\frac{2\Delta P}{\rho_l}} = \frac{\dot{m}_{\text{inj}}}{A_n \rho_l}, \quad (2)$$

$$t_b = 4.351 \sqrt{\frac{2\rho_l}{\rho_g}} \frac{d_n}{C_d u_{\text{inj}}}, \quad (3)$$

where $C_d$ is the injector nozzle discharge coefficient, $\Delta P$ is the pressure drop across injector nozzle, $\rho_l$ is the density of liquid fuel, $\rho_g$ is the density of gaseous fuel, $\dot{m}_{\text{inj}}$ is the injection mass flow rate, $A_n$ is the injector nozzle area, and $d_n$ is the injector nozzle coefficient [8].

## 2.2 Entrainment

As the fuel spray is injected into the combustion chamber, it is slowed down by the entrainment of unburned and burned gases into the spray. The injection pulses are mixed together through entrainment. Each packet has its own position and velocity that are determined by an empirical correlation for spray tip penetration described in refs [9] and [10]. The entrainment rate is based on the conversation of momentum

$$m_{\text{inj}} u_{\text{inj}} = (m_{\text{inj}} + m_{\text{air-entrained}}) u, \quad (4)$$

where $u = \mathrm{d}S/\mathrm{d}t$ is the final velocity of the entrained air-fuel mixure, $m_{\text{inj}}$ is the initial mas of the injected fuel packet, and $m_{\text{air-entrained}}$ is the entrained air mass of the packet.

The left-hand side of equation (4) represents the initial spray momentum and right-hand side final entrainment mixure momentum. $m_{\text{air-entrained}}$ is dependent on injection velocity

$$m_{\text{air-entrained}} = \frac{m_{\text{inj}} u_{\text{inj}}}{u}. \quad (5)$$

The rate of entrained fuel–gas mixture is defined as

$$\frac{\mathrm{d}m}{\mathrm{d}t} = -C_{\text{ent}} \frac{m_{\text{inj}} u_{\text{inj}}}{u^2} \frac{\mathrm{d}u}{\mathrm{d}t}, \quad (6)$$

where $C_{\text{ent}}$ is the entrainment rate multiplier [8].

## 2.3 Evaporation

The droplet evaporation model used in DI-pulse is based on the works of refs [11] and [12]. The energy balance around the droplet is shown in equation (7)

$$m_d c_{pd} \frac{\mathrm{d}T}{\mathrm{d}t} = \frac{\mathrm{d}Q_c}{\mathrm{d}t} + \frac{\mathrm{d}Q_e}{\mathrm{d}t}, \quad (7)$$

where $m_d$ is the mass of the droplet and $c_{pd}$ is the specific heat capacity of the droplet. The rate of convective heat transfer is defined as

$$\frac{\mathrm{d}Q_c}{\mathrm{d}t} = h\pi d_d^2 (T_g - T_d), \quad (8)$$

where $d_d$ is the diameter of the droplet, $T_g$ is the temperature of the entrained gas, and $T_d$ is the temperature of the droplet.

The absorbed heat from the control volume due to the enthalpy change is defined as

$$\frac{\mathrm{d}Q_e}{\mathrm{d}t} = -\frac{\mathrm{d}m_d}{\mathrm{d}t} \Delta H_{vd}, \quad (9)$$

where $\mathrm{d}m_d/\mathrm{d}t$ is the rate of the evaporation of the droplet and $\Delta H_{vd}$ is the latent heat of vaporization of the droplet.

## 2.4 Ignition delay

The mixture of each pulse is affected by an ignition delay, which is modeled with an Arrhenius equation as shown in equation (10) [13]. Each injection pulse has its own ignition delays, which is based on the conditions within the pulse, i.e. entrainment and evaporation within the pulse in addition to pulse-to-pulse interactions.

$$\tau_{\text{ign}} = C_{\text{ign}} \rho^{-1.5} e^{\left(\frac{3500}{T}\right)} [O_2]^{-0.5}, \quad (10)$$

where $C_{\text{ign}}$ is the ignition delay multiplier, $\rho$ is the density of the pulse gas, $T$ is the temperature of the pulse, and $[O_2]$ is the concentration of the oxygen. Ignition occurs when

$$\int_{t_{\text{SOI}}}^{t_{\text{SOC}}} \frac{1}{\tau_{\text{ign}}} \mathrm{d}t = 1, \quad (11)$$

where $t_{\text{SOI}}$ is the time at the start of injection (SOI) and $t_{\text{SOC}}$ is the time at the start of combustion (SOC).

## 2.5 Premixed combustion

Once an injection pulse is ignited, the mixture present at the time is set aside for premixed combustion. The rate of premixed combustion is set to be kinetically limited and can be modified by premixed combustion rate multiplier ($C_{pm}$). The rate of premixed combustion is defined as

$$\frac{\mathrm{d}m_{pm}}{\mathrm{d}t} = C_{pm} m_{pm} k (t - t_{\text{SOC}})^2 f(\cdot), \quad (12)$$

where $m_{pm}$ is the premixed mass, $k$ is the turbulent kinetic energy, and $t$ is the time after the injection. $f(\cdot)$ indicates that the premixed combustion depends on other factors such as temperature, concentration of oxygen, EGR fraction, air-fuel ration, and the kinetic rate constant [8].

## 2.6 Diffusion combustion

The remaining unmixed fuel and entrained gas after the ignition continue to mix and burn in a primarily diffusion-limited phase. The rate of diffusion combustion can be adjusted by the diffusion combustion rate multiplier ($C_{df}$). The diffusion combustion rate is presented in equation (13)

$$\frac{\mathrm{d}m}{\mathrm{d}t} = C_{df} m \frac{\sqrt{k}}{\sqrt[3]{V_{\text{cyl}}}} f(\cdot), \quad (13)$$

where $V_{\text{cyl}}$ is the cylinder volume. The rate of the diffusion combustion is small at high loads due to spray wall and spray–spray interactions. $f(\cdot)$ is the same as in equation (12) [6].

# 3 Engine simulations

The engine runs at speed mode, where the user enters the speed and the engine torque is calculated. The simulation will run until it reaches a steady state for each case. Cases contain high and low load at different speeds. The

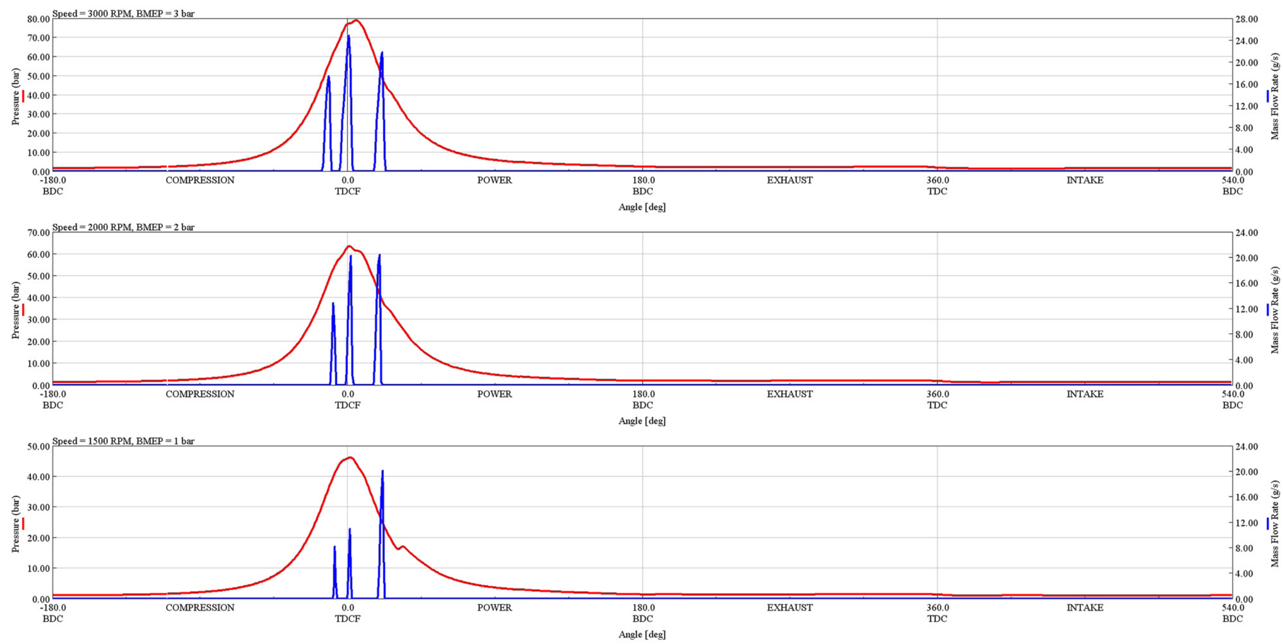


**Figure 2:** Cylinder pressure trace (red) with respect to injection pulses (blue).

number of cycles varies from 25 to 100. Three injections are used for the combustion, pilot (also known as pre), main, and post injection.

The cylinder pressure trace with respect to injection pulses is shown in Figure 2. The results are from three simulation runs with different speed and low load.

The pilot, main, and post injections are shown in Figure 2 starting from left to right, respectively. The idea is to maintain maximum pressure as long as possible. The purpose of pilot injection is reducing combustion noise. Post injection is added to reduce the formation of soot [14]. For the purpose of the system identification and MPC design in this work, it was enough to run the simulation for one operating point. The model was run at a speed of 3,000 rpm and a brake mean effective pressure of 3 bar. The SOI and injected fuel mass of pilot and main were kept within a narrow range, while SOI and injected fuel mass of post injection were run as a sweep. Injected fuel mass for the main injection was kept constant. The detailed values of each injection are presented in Table 1.

Values of the SOI for pilot and main injections are obtained from injection profiles. The results of the simulations, i.e., SOI and injected fuel mass, and maximum cylinder pressure and IMEP are used to estimate the state-space representation of the engine model with system identification. The state-space model is controlled with the designed MPC.

# 4 System identification for state-space estimation

Designing an MPC controller requires an estimated state-space representation of the process plant. In this work, the cycle to cycle combustion process is modeled in a form of a simple state-space model as in equation (14), where $X(k)$ and $Y(k)$ are the system states and outputs, $U(k)$ is the input. $A$, $B$, and $C$ are the system and system input and output matrices.

$$\begin{aligned} X(k+1) &= AX(k) + BU(k) \\ Y(k) &= CX(k). \end{aligned} \tag{14}$$

Instead of using the post injection timing, $SOI_{post}$, directly as one of the input, a relative distance between the main, $SOI_{main}$, and the post injection timing is taken into account as in equation (15)

**Table 1:** Values of injections for each cycle

| Injection | SOI (∘) | mf (mg) |
|---|---|---|
| Pilot | −3.6 … − 2.6 | 1 … 5 |
| Main | 0 … 1 | 50 |
| Post | 12 … 24 | 4 … 5 |

$$\mathrm{dSOI} = \mathrm{SOI}_{\mathrm{post}} - \mathrm{SOI}_{\mathrm{main}}. \tag{15}$$

Similarly, injected mass of the post injection, $m_{\mathrm{post}}$, is also replaced as an input by a ratio (rp) of the mass of the post injection to the total mass injected (equation (16))

$$\mathrm{rp} = \frac{m_{\mathrm{post}}}{(m_{\mathrm{post}} + m_{\mathrm{main}})}. \tag{16}$$

Outputs of the model are decided to be the maximum cylinder pressure ($p_{\mathrm{max}}$) and the brake specific fuel consumption (BSFC). The state equation of the state-space model then has a form of

$$\begin{bmatrix} p_{\mathrm{max}}(k+1) \\ \mathrm{BSFC}(k+1) \end{bmatrix} = A \begin{bmatrix} p_{\mathrm{max}}(k) \\ \mathrm{BSFC}(k) \end{bmatrix} + B \begin{bmatrix} \mathrm{dSOI}(k) \\ \mathrm{rp}(k) \end{bmatrix}, \tag{17}$$

where the assumption of a static relation between $U$ and $X$ gives $A = I_{2\times 2}$ (identity matrix) and leaves $B$ to be determined by a linear regression. Moreover, matrix $C$ in equation (14) is also given as $I_{2\times 2}$. Data used in the system identification are collected from running a set of designed simulation in the aforementioned GT-suite multi-injection engine model.

To form a linear regression for $B$, equation (20) then becomes

$$\begin{bmatrix} \Delta_{p_{\mathrm{max}}(k+1)} \\ \Delta_{\mathrm{BSFC}(k+1)} \end{bmatrix} = B \begin{bmatrix} \mathrm{dSOI}(k) \\ \mathrm{rp}(k) \end{bmatrix}, \tag{18}$$

where

$$\begin{aligned} \Delta_{p_{\mathrm{max}}(k+1)} &= p_{\mathrm{max}}(k+1) - p_{\mathrm{max}}(k), \\ \Delta_{\mathrm{BSFC}(k+1)} &= \mathrm{BSFC}(k+1) - \mathrm{BSFC}(k). \end{aligned} \tag{19}$$

Denote that

$$\Delta = \begin{bmatrix} \Delta_{p_{\mathrm{max}}(k+1)} \\ \Delta_{\mathrm{BSFC}(k+1)} \end{bmatrix}, \quad U = \begin{bmatrix} \mathrm{dSOI}(k) \\ \mathrm{rp}(k) \end{bmatrix}.$$

Hence by using linear regression, matrix $B$ is formed as

$$B = \Delta \times U^T \times (UU^T)^{-1}. \tag{20}$$

# 5 MPC

The controller in this work is developed based on the theory in ref. [5]. The cycle to cycle model in equation (21) is rewritten for easier notation as

$$\begin{aligned} x_m(k+1) &= A_m x_m(k) + B_m u(k) \\ y(k) &= C_m x_m(k). \end{aligned} \tag{21}$$

Taking denote the difference of the state variable and the control variable as

$$\begin{aligned} \Delta x_m(k+1) &= x_m(k+1) - x_m(k) \\ \Delta x_m(k) &= x_m(k) - x_m(k-1) \\ \Delta u(k) &= u(k) - u(k-1). \end{aligned} \tag{22}$$

The difference of the state space equation is

$$\Delta x_m(k+1) = A_m \Delta x_m(k) + B_m \Delta u(k). \tag{23}$$

The state variable $\Delta x_m(k)$ is connected to the output $y(k)$ by choosing a new state variable vector

$$x(k) = [\Delta x_m(k)^T y(k)^T] \tag{24}$$

and the difference equation of the output is

$$\begin{aligned} y(k+1) - y(k) &= C_m(x_m(k+1) - x_m(k)) \\ &= C_m \Delta x_m(k+1) \\ &= C_m A_m \Delta x_m(k) + C_m B_m \Delta u(k). \end{aligned} \tag{25}$$

Combining equation (23) and equation (25) gives the following augmented state-space model

$$\begin{aligned} \begin{bmatrix} \Delta x_m(k+1) \\ y(k+1) \end{bmatrix} &= \begin{bmatrix} A_m & 0 \\ C_m A_m & I \end{bmatrix} \begin{bmatrix} \Delta x_m(k) \\ y(k) \end{bmatrix} + \begin{bmatrix} B_m \\ C_m B_m \end{bmatrix} \Delta u(k), \\ y(k) &= [0 \quad I] \begin{bmatrix} \Delta x_m(k) \\ y(k) \end{bmatrix}, \end{aligned} \tag{26}$$

where $I$ and 0 are, respectively, the identity and zero matrix with dimension $m \times m$, where $m$ is the number of inputs. Based on the augmented state space, the future state variables are calculated sequentially for a $N_p$ number of samples (called prediction horizon) and within a control horizon $N_c$ which is chosen to be less than (or equal) to the prediction horizon $N_p$. Define the vectors $Y$ and $\Delta U$ as:

$$\begin{aligned} \Delta U &= [\Delta u(k_i)^T \; \Delta u(k_i+1)^T \; \ldots \; \Delta u(k_i + N_c - 1)^T]^T \\ Y &= [y(k_i+1)^T \; y(k_i+2)^T \; \ldots \; y(k_i + N_p)^T]^T. \end{aligned} \tag{27}$$

A general formula for future state variable prediction is

$$Y = Fx(k_i) + \Phi \Delta U, \tag{28}$$

where $F$ and $\Phi$ matrices are defined as in ref. [5]. Assuming that the set-point is defined as $R_s^T$, the controller aims to minimize the cost function $J$ with the corresponding $\Delta U$

$$J = (R_s - Y)^T (R_s - Y) + \Delta U^T \bar{R} \Delta U, \tag{29}$$

in which $\bar{R}$ is a weighting matrix of a form $\bar{R} = r_w \times I_{N_c \times N_c} (r_w \geq 0)$, where $r_w$ is used as a tuning parameter for the controller performance. The optimal solution for the control signal $\Delta U$ is

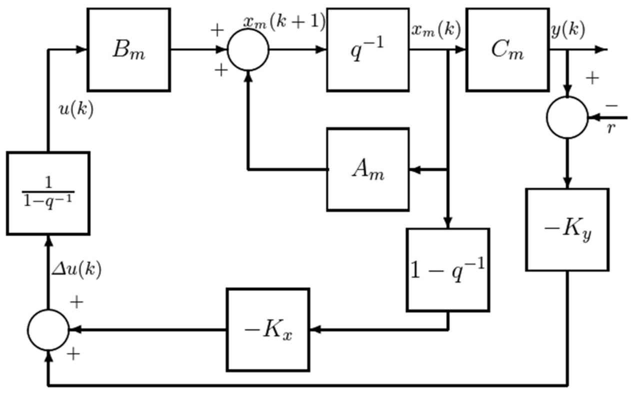


**Figure 3:** Closed-loop control system of MPC [5].

$$\Delta U = (\Phi^T \Phi + \bar{R})^{-1} \Phi^T (R_s - Fx(k_i)). \tag{30}$$

Applying the receding horizon control principle, the first $m$ elements (where $m$ is the number of inputs) in $\Delta U$ are taken to form the incremental optimal control

$$\begin{aligned} \Delta u(k_i) &= [I_m \; 0_m \; \ldots \; 0_m](\Phi^T \Phi + \bar{R})^{-1} \Phi^T (R_s - Fx(k_i)), \\ &= K_y r(k_i) - [K_x \quad K_y] x(k_i). \end{aligned} \tag{31}$$

## 6 Results

The controller is implemented in a closed-loop control system for verification. The control scheme is depicted in Figure 3.

The simulation of the above control scheme is conducted in MATLAB, and Figure 4 shows the testing results. The reference values for $P_{max}$ and BSFC are set to be 85 bar and 320 g/kW h, respectively.

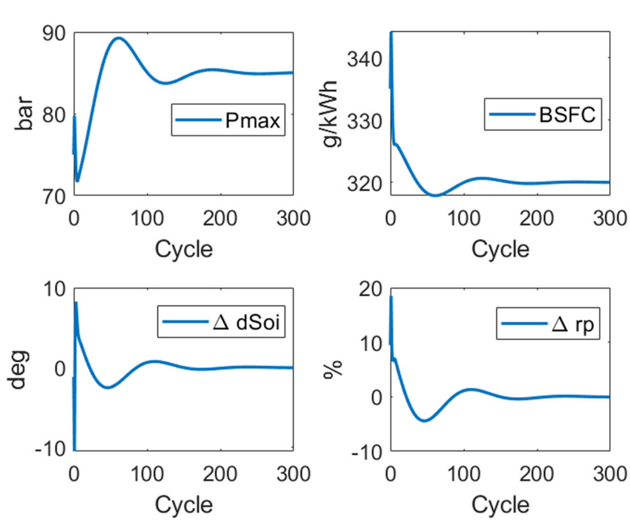


**Figure 4:** Simulation results.

As can be seen from the plot, the controller reacts to the changes in the inputs and maintains the outputs at desired values. The upper two plots show the outputs which stabilize and reach the desired values after around 200 cycles.

The lower plots demonstrate the control signals $\Delta u(k_i)$ of the MPC. In the beginning of the cycles, the control signals reach negative values at times which shows that the main injection is overlapped by the post injection although the controller stabilizes towards the end. This is potentially caused by several reasons such as the uncertainties in modeling, the lack of constraints of the control signals, etc. Hence, there are more room for improvements in the future work.

## 7 Conclusion

In this work, an MPC controller is developed for a multiple injection combustion model. The main goal was to control post injection of the engine model to obtain the desired BSFC and maximum cylinder pressure. This was achieved by creating a state-space model for engine with system identification. The data required for the system identification were obtained from a phenomenological engine model developed by Gamma Technologies. This proved that simulation models can provide data as sufficient as from a real engine run. The estimated state-space model of the engine was then used as a process model for the MPC controller. The results indicate that it is possible to implement a closed-loop control system purely from data generated by a simulation model.

**Acknowledgements:** The research was carried out in cooperation with Wärtsilä Marine Solutions in the project "Integrated Energy Solutions to Smart and Green Shipping" (INTENS) funded by Business Finland.

**Conflict of interest:** Authors state no conflict of interest.

**Data Availability Statement:** Authors have collected the data by using the simulation software and the data is stored within the research group. It can be accessible upon request.

## References

[1] Nguyen Khac H, Zenger K, Storm X, Hyvönen J. Operational profile based optimization method for maritime diesel

engines. Energies. 2020;13(10):1–21. doi: 10.3390/en13102575.
[2] Turesson G. Model-based optimization of combustion-engine control. PhD thesis, Lund University, Sweden, June 2018. doi: 10.13140/RG.2.2.36319.97440.
[3] Yamasaki Y, Ikemura R, Takahashi M, Shimizu F, Kaneko S. Simple combustion model for a diesel engine with multiple fuel injections. Int J Eng Res. 2019;20(2):167–80.
[4] Mendez S, Thirouard B. Using multiple injection strategies in diesel combustion: Potential to improve emissions, noise and fuel economy trade-off in low cr engines. SAE Int J Fuels Lubr. April 2008;1:662–74. doi: 10.4271/2008-01-1329.
[5] Wang L. Model predictive control system design and implementation using MATLAB. London: Springer; 2009. doi: 10.1007/978-1-84882-331-0.
[6] Gamma Technologies. The standard in multi-physics system simulation; USA.
[7] Payri R, Salvador FJ, Martí-Aldaraví P, Martínez-López J. Using one-dimensional modeling to analyse the influence of the use of biodiesels on the dynamic behavior of solenoid-operated injectors in common rail systems: detailed injection system model. Energy Conv Manag. 2012;54(1):90–9.
[8] Gamma technologies. Engine performance application manual, USA; 2017.
[9] Kumar G, Kumar A. Spray behavior comparison in diesel engine with biodiesel as fuel. J Energy Technol Policy. 2013;3(4):14–24.
[10] Jung D, Assanis DN. Multi-zone di diesel spray combustion model for cycle simulation studies of engine performance and emissions. In: SAE Technical Paper. SAE International; March 2001.
[11] Aggarwal S, Peng F. A review of droplet dynamics and vaporization modeling for engineering calculations. J Eng Gas Turbines Power-Trans Asme. 1995;117:453–61.
[12] Prommersberger K, Maier G, Wittig S. Validation and application of a droplet evaporation model for real aviation fuel. RTO Meeting Proceedings; 1999.
[13] Livengood JC, Wu PC. Correlation of autoignition phenomena in internal combustion engines and rapid compression machines. Symp (Int) Combust. 1955;5(1):347–56.
[14] Badami M, Mallamo F, Millo F, Rossi EE. Influence of multiple injection strategies on emissions, combustion noise and bsfc of a di common rail diesel engine. In: SAE Technical Paper. SAE International; Match 2002. doi: 10.4271/2002-01-0503.